

# Dose reconstruction in the OCTAVIUS 4D phantom and in the patient without using dose information from the TPS

B. Allgaier, E. Schüle, J. Würfel

PTW-Freiburg Physikalisch-Technische Werkstätten Dr. Pychlaus GmbH  
Lörracher Straße 7, 79115 Freiburg, Germany

## 1. Introduction

Intensity modulated radiation therapy (IMRT) and volumetric modulated arc therapy (VMAT) are state-of-the-art irradiation techniques for the delivery of highly conformal radiation fields to the target volume. These techniques require complex treatment planning system (TPS) algorithms as well as sophisticated irradiation methods. As a result, the use of quality assurance tools for the verification of the planned dose distribution prior to the treatment of the patient has become a standard procedure in clinical routine.

Early quality assurance (QA) tools for this purpose are two-dimensional devices based on stationary 2D detector panels [1], [2], [3], [4], [5]. They allow the measurement of one plane of dose values in order to compare it with the corresponding plane calculated by the TPS. Some of these tools have restrictions regarding the angle of the incident beam because of the angular dependence of the detector panel [4], requiring so-called collapsed beam measurements during which the gantry of the treatment unit is fixed at a certain angle. Other tools allow composite plan measurements by correcting for the directional dependence either by the application of correction factors [1], [5], or by the use of suitably shaped phantoms [3].

Because of the complex volumetric shape of the highly conformal fields the limitation to one measuring plane is considered a disadvantage. Ideally, a full 3D dose matrix is desirable. To date the only realistic 3D dosimetry system is based on gel dosimetry [6], but unfortunately there are restrictions in the use of such systems in clinical routine such as the availability of gels with reproducible features, temperature dependence, the change of the irradiated gel volume by time as well as the necessity of relatively complex equipment for the evaluation of the irradiated gel samples.

As an alternative to real three-dimensional radiation detectors 2D detector panels can be used for the dose

measurements, combined with a dose reconstruction method that determines dose values in the 3D volume. Such 2D detectors are available either as planar detector panels [7], [8], [9] or as the surface of a cylinder [10]. All these systems measure time-resolved dose values at a limited number of positions and reconstruct 3D dose values in the complete volume. While some systems [7], [9] perform this task as independent measuring tools other systems [8], [10] require the dose distribution calculated by the TPS as an input for the dose reconstruction. Many clinical physicists prefer QA tools to be independent of the object to be tested. Therefore, the OCTAVIUS 4D was designed as a truly independent tool for pre-treatment quality assurance. This paper describes the algorithms on which the OCTAVIUS 4D dose reconstruction in the phantom and in the patient are based. In addition, some of the results of the system verification are presented.

## 2. 3D dose reconstruction methods

### 2.1 TPS dependent methods

One example of a QA system for 3D dose measurements is ArcCHECK with 3DVH option [10]. The ArcCHECK detectors are located in a plane that forms the surface of a cylinder, allowing the radiation beam to hit at least the central detectors perpendicularly at any gantry angle. Dose reconstruction in the entire volume of the cylinder is based on the modification of the dose matrix calculated by the TPS. Therefore, before ArcCHECK can determine the volumetric dose grid, the treatment plan including its dose values needs to be entered into the ArcCHECK software. Then the TPS data are “corrected” by the measured values, and the corrected TPS data are presented as the ArcCHECK measuring result. This method is called “ArcCHECK Planned Dose Perturbation” (ACPDP) [10]. The scaling factors for the perturbation of the plan are interpolated from the measured entry and exit values of the phantom, resulting in a “morphing” of the dose grid rather than a simple re-normalization. In order to determine the

dose distribution in the patient, the correction factors obtained for the phantom are simply used for the calculated patient plan as well, ignoring the patient size and structure [10]. In summary, the ArcCHECK method for dose reconstruction is based on the calculated treatment plans for the phantom and for the patient. Without the import of TPS dose data, ArcCHECK is not able to present 3D dose grids. Therefore, the ArcCHECK method cannot be considered to be independent of the treatment plan that is to be verified.

In a similar way, the Delta-4 [8] system requires the input of dose information from the TPS in order to establish a 3D dose grid. The Delta-4 modifies the treatment plan analogously to ArcCHECK.

## 2.2 Stand-alone methods

Stand-alone QA tools do not use the dose grid calculated by the TPS in order to determine measured dose distributions in the phantom or in the patient, they need the TPS dose grid only for the comparison with the measurements.

Examples for stand-alone systems are COMPASS [9] and OCTAVIUS 4D [7], [12]. While the COMPASS algorithm is more complex and constitutes a treatment planning system on its own [11], the OCTAVIUS 4D algorithm is very straight forward and requires only few fundamental input data, i.e. percentage depth dose curves (PDDs) for different field sizes.

The basic version of OCTAVIUS 4D reconstructs dose grids in the phantom. The optional “DVH 4D” algorithm allows dose volume histograms in the patient to be calculated.

## 3. OCTAVIUS 4D dose reconstruction

### 3.1 Data acquisition with OCTAVIUS 4D

The OCTAVIUS 4D phantom (Fig. 1) rotates synchronously with the gantry, taking time- and gantry angle-resolved dose measurements. In the course of the measurements the complete phantom volume is covered by measuring points. Depending on the application, detector panels with different spatial resolution can be used in the rotational phantom. The beam incidence is always perpendicular to the surface of the detector panel, avoiding the need of angular correction factors. The data is collected and evaluated by means of the VeriSoft software package that is part of the OCTAVIUS 4D system.

Data is accumulated over measuring intervals of 200 ms. This measuring interval is considered the best compromise between most accurate dose data and optimal correlation between dose and gantry angle values. Integrating data over 200 ms results in a high signal-to-noise ratio and dose values that do not need further smoothing. In this context, the use of ionization chambers instead of silicon diodes is advantageous as chambers usually have a better signal-to-noise ratio by design. On the other hand, a 200 ms

measuring interval ensures a good correlation between the dose data and the gantry angles. Assuming the currently highest gantry speed of 360° per minute, the uncertainty of the gantry angle due to the 200 ms measuring interval arises to  $\pm 0.6^\circ$ . Combining this value with the inherent uncertainty of the inclinometer of  $\pm 1^\circ$  leads to a total uncertainty of the gantry angle for the 3D dose reconstruction algorithms of  $\pm 1.2^\circ$  at a gantry speed of 360° per minute. Radiological tests of the inclinometer's accuracy can be found in the literature [7], [12].

During a typical VMAT measurement over two minutes OCTAVIUS 4D directly measures more than 400,000 dose points, distributed over the cylindrical volume of the phantom.

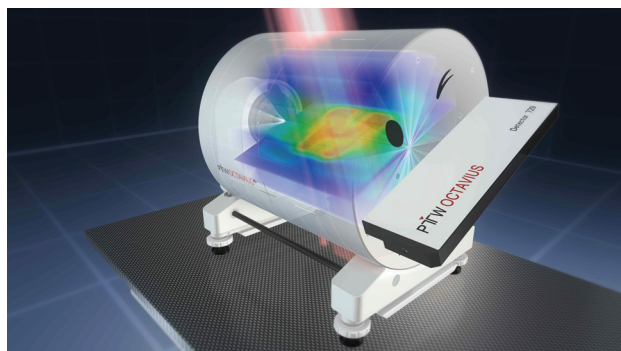


**Fig. 1** The OCTAVIUS 4D system. The detector panel is inserted in a cylindrical phantom that rotates synchronously with the gantry. Detector panels with different spatial resolutions are available. The Detector 729 features 10 mm resolution, the central region of the Detector 1000<sup>SRS</sup> features 2.5 mm.

### 3.2 Commissioning of OCTAVIUS 4D

The OCTAVIUS 4D algorithm is based on dose measurements at a certain depth in the phantom and on percentage depth dose curves (PDDs) that are used to reconstruct dose values along the ray lines that connect the relevant detectors and the focus of the beam. As a consequence, the commissioning of OCTAVIUS 4D is very simple and limited to PDD measurements and to the adjustment of the phantom's density in the TPS.

For commissioning, PDDs should be measured in a water phantom at a source-to-surface-distance of 85 cm. PDDs for field sizes of 4 x 4 cm<sup>2</sup>, 10 x 10 cm<sup>2</sup> and 26 x 26 cm<sup>2</sup> are mandatory, additional field sizes may slightly improve the accuracy of the reconstruction algorithms.

In the TPS, the electron density of the OCTAVIUS 4D phantom relative to water should be set to 1.016. If this is not supported by the TPS, the phantom's mass density or the corresponding Hounsfield Unit used by the TPS is to be adjusted in accordance with the manufacturer's suggested procedure [13]. The phantom can be imported into the TPS by using the artificial CT file provided with the OCTAVIUS 4D system, or by performing a CT scan without the detector panel in place.

### 3.3 Dose distribution in the OCTAVIUS 4D phantom

OCTAVIUS 4D and its associated software VeriSoft are designed to measure and reconstruct a 3D dose grid without using dose information from the treatment planning system. Therefore, the measuring results of the QA test tool are completely independent of the treatment plan. The basics of the 3D dose reconstruction algorithm are easy to understand:

- a) Convert the PDDs measured in water upon commissioning to PDDs in the OCTAVIUS 4D phantom, using the known relation of the electron densities of water and phantom material
- b) At the current gantry angle (time) consider one detector of the detector panel ("current detector")
- c) Measure the dose  $D_{Det}$  in Gy at this position
- d) Construct a ray line through the current detector to the focus of the beam
- e) Determine the current field size from the irradiated detectors
- f) Apply corrections for non-central-axis TPRs according to [14] in case of beams with flattening filter, or according to [15] in case of flattening filter free (FFF) beams
- g) Inside the phantom, using the PDD appropriate for the current field size, reconstruct dose values  $D(r)$  in Gy at the distance  $r$  from the current detector along the ray line according to equation (1)
- h) Do this for all detectors of the detector panel
- i) Do this for all gantry angles
- j) Sort all of the dose values obtained this way into voxels of  $2.5 \times 2.5 \times 2.5 \text{ mm}^3$  (can be changed by the user) by linear interpolation
- k) For the Detector 729, remove a layer of 3 cm in thickness from the outer shell of the phantom to obtain a dose grid in a cylinder with 26 cm in diameter and 26 cm in length. For the Detector 1000<sup>SRS</sup> the reconstructed cylinder is 11 cm in diameter and 11 cm in length.

The dose  $D(r)$  along a ray line is obtained from the dose  $D_{Det}(0)$ , measured by the current detector, using the following relationship

$$D(r) = D_{Det}(0) \cdot \frac{PDD(r)}{PDD(0)} \quad (1)$$

where  $PDD(r)$  and  $PDD(0)$  are the percentage depth dose values at the distance  $r$  from the current detector and at the position of the current detector, respectively.

The outer shell of the phantom is removed from the reconstructed data as in this region no detectors exist. Scattered radiation is accounted for by the detectors surrounding the current detector. For a typical VMAT plan approximately 1.1 million voxels (dose points) are

reconstructed this way. The dose reconstruction time needed by OCTAVIUS 4D is approximately 25 s.

### 3.4 Dose distribution in the patient

In order to reconstruct the 3D dose distribution in the patient, the CT data containing the densities of the structures must be imported into VeriSoft. The patient dose reconstruction follows the steps described in chapter 3.3, however with a different procedure in step g). In contrast to the phantom, the patient is not homogeneous along the ray line but features structures with different densities. Also, the source-to-surface-distance differs because of the irregular shape of the patient contour. This situation is depicted in Fig. 2.

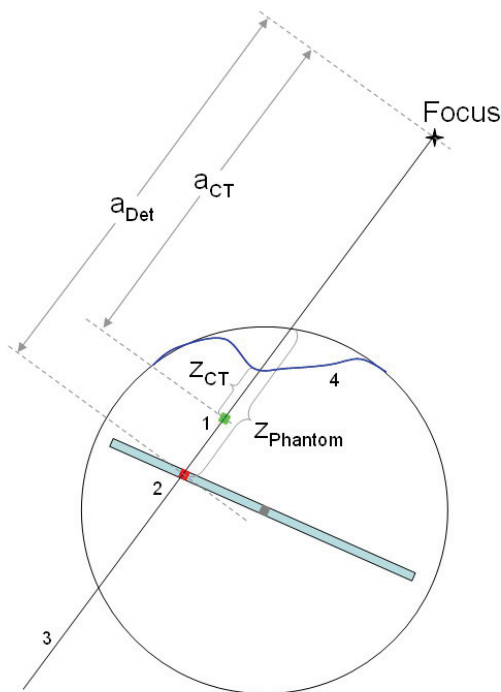


**Fig. 2** OCTAVIUS 4D phantom with ray line (3) through focus and current detector (2), not to scale. The contour (4) is the patient surface from the CT image. The current detector measures the dose  $D_{Det}$  at the water-equivalent depth  $z_{Phantom}$ . The algorithm reconstructs the dose  $D_{CT}$  for the current voxel (1) at the water-equivalent depth  $z_{CT}$  in the CT image.  $a_{Det}$  and  $a_{CT}$  are geometrical distances from the focus to the current detector and to the current voxel, respectively.

To determine the patient dose at a point on the ray line, a relationship between the dose measured in the phantom by the current detector,  $D_{Det}$ , and the dose at the point on the ray line in the CT image,  $D_{CT}$ , is established. The steps of the algorithm are:

- g.1) Convert the PDDs to tissue-phantom-ratios (TPRs)
- g.2) Select a point ("current voxel") on the ray line constructed in d)
- g.3) Along the ray line, convert the Hounsfield units from the CT to electron densities [16]

- g.4) Determine the water-equivalent depth of the current detector in the phantom,  $z_{Det}$ , by multiplication of the geometric depth with the ratio of the electron densities of the phantom material and water
- g.5) Determine the water-equivalent depth of the current voxel in the patient,  $z_{CT}$ , according to equation (3)
- g.6) Determine the geometrical distances between focus and current voxel,  $a_{CT}$ , and between focus and current detector,  $a_{Det}$
- g.7) Calculate the dose in the patient  $D_{CT}$  at the current voxel by application of equation (2)
- g.8) Do this for all voxels along the ray line inside the patient's contour.

The reconstruction of the dose in the patient (or in the CT image) along a ray line through the current detector and the focus is based on equation (2). The meaning of the symbols is explained above.

$$D_{CT} = D_{Det} \cdot \frac{TPR(z_{CT})}{TPR(z_{Det})} \cdot \left( \frac{a_{Det}}{a_{CT}} \right)^2 \quad (2)$$

The first term in equation (2) accounts for different thicknesses of overlaying material in front of the current detector in the phantom and in front of the current voxel in the patient (or CT). The water-equivalent depth  $z_{CT}$  of the current voxel in the patient is obtained from the geometrical depth  $z_{CT}^{geom}$  and the electron densities of the materials involved:

$$z_{CT} = z_{CT}^{geom} \cdot \frac{\sum_{i=1}^n \rho_{CT,i}}{n \cdot \rho_{Water}} \quad (3)$$

where  $n$  is the number of voxels along the ray line from the current voxel to the surface of the patient,  $\rho_{Water}$  is the electron density of water, and  $\rho_{CT,i}$  is the electron density of voxel  $i$  ( $i = 1, 2, \dots, n$ ).

The second term in equation (2) accounts for the different distances to the focus by applying the inverse square law.

The TPRs in equation (2) are transformed from the measured PDDs by application of the inverse square law according to BJR 11 [17].

This algorithm is not able to account for the change of scattered radiation as the position on the ray line passes structures with different density.

The time needed by OCTAVIUS 4D to reconstruct the 3D dose distribution in the patient is typically in the order of two minutes.

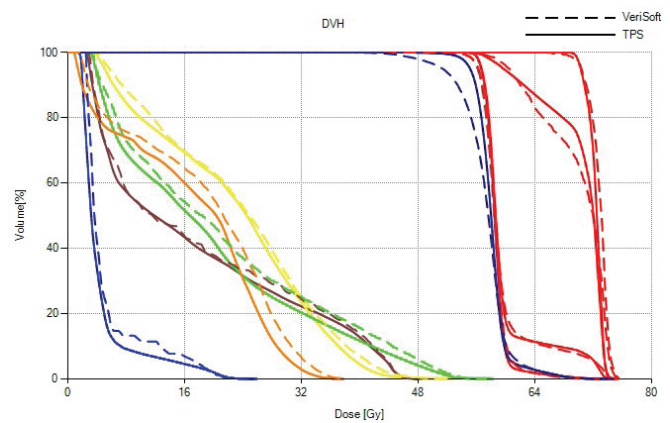


**Fig. 3** Dose volume histograms in the patient's geometry determined by OCTAVIUS 4D (dashed lines) and by the TPS (solid lines)

Mostly, dose distributions in the patient are visualized by means of dose volume histograms (DVHs). Usually, DVHs are presented not for the complete patient but for different structures such as organs at risk or target volumes. In order to determine DVHs the VeriSoft software must import the geometry of the patient structures from the TPS. The DVH algorithm uses the reconstructed 3D dose distribution in the patient and determines the histograms from the dose values inside the structures. VeriSoft only considers structures that are completely inside the OCTAVIUS 4D measuring volume. If the TPS allows DVH curves to be exported, they can be compared with the DVH curves determined by OCTAVIUS 4D as depicted in Fig. 3.

## 4. Reconstruction accuracy

### 4.1 Test methods

The absolute accuracy of systems like OCTAVIUS 4D is hard to determine for all clinical situations. Besides other parameters, the accuracy depends on the complexity of the treatment plan, on the presence of dose gradients and regions of low density, and on the spatial resolution of the detector panel used for the measurements. For this paper, two methods were chosen to estimate the accuracy of the measured dose distribution in the phantom: comparison of static field results with TPS calculations (chapter 4.2), and comparison of complex clinical IMRT and VMAT plans with the results of a treatment planning system, as well as with measurements obtained by a stationary OCTAVIUS II system (chapter 4.3).

The accuracy of the DVHs was also tested employing two different methods. First, the reconstructed maximum dose in the patient was compared with the TPS dose calculation. Second, a full-volume gamma analysis on the reconstructed dose volume was performed by comparison with the treatment plan (chapter 4.4).

Before the measurements and the data analysis the OCTAVIUS 4D system was correctly commissioned as described in chapter 3.2. Special attention was given to the correct adjustment of the phantom's electron density in the treatment planning system.

Unless otherwise noted, all comparisons of dose distributions were made with VeriSoft 6.0 in form of a 3D gamma analysis with a local gamma criterion of 3% / 3 mm, suppression of dose values below 10% of the maximum dose, and with the "2<sup>nd</sup> and 3<sup>rd</sup> pass" option activated [18]. In the following, the relative number of voxels that pass this gamma criterion is referred to as "pass rate" and serves as a measure for the goodness of the reconstructed dose distribution.

The measurements were made on a Varian Clinac iX linear accelerator and compared with the treatment plans created by the Varian Eclipse V10 treatment planning system. A comprehensive verification of the OCTAVIUS 4D system can also be found in the literature [7], [12].

#### 4.2 Comparison with static fields

A simple way to get an idea of the accuracy of the implemented algorithm is the application of a static field to the OCTAVIUS 4D, and the comparison of the reconstructed cross profiles and the reconstructed depth profile with the corresponding profiles obtained from the TPS. It can be assumed that the accuracy of the TPS for such a simple geometry is good enough to serve as reference. Figures 4 - 6 show the results of a static 10 x 10 cm<sup>2</sup> beam evaluated with OCTAVIUS 4D. It can be seen from Fig. 4 that with the standard detector panel (Detector 729) the profiles show deviations in the penumbra regions because of the panel's spatial resolution of 10 mm. These deviations, however, become less important as the beam rotates, averaging over many measuring angles and smearing out the resolution effect. This was demonstrated by the measurement of a full arc irradiation using the same field, resulting in a cylindrical dose distribution that matched the distribution calculated by the TPS with a pass rate of 99.8% as compared to 83.3% for the static field.

Using a detector panel with higher spatial resolution such as the OCTAVIUS Detector 1000<sup>SRS</sup> almost eliminates the resolution effect even for static beams. The spatial resolution in the central area (5.5 x 5.5 cm<sup>2</sup>) of this detector panel is 2.5 mm, and the pass rate obtained was 100%. As a result, the measured profiles are in very good agreement with the TPS profiles (Fig. 5).

Fig. 6 depicts a 6 MV depth dose curve obtained with the OCTAVIUS 4D with Detector 729, applying a static 10 x 10 cm<sup>2</sup> field. The conformance with the TPS is very good.

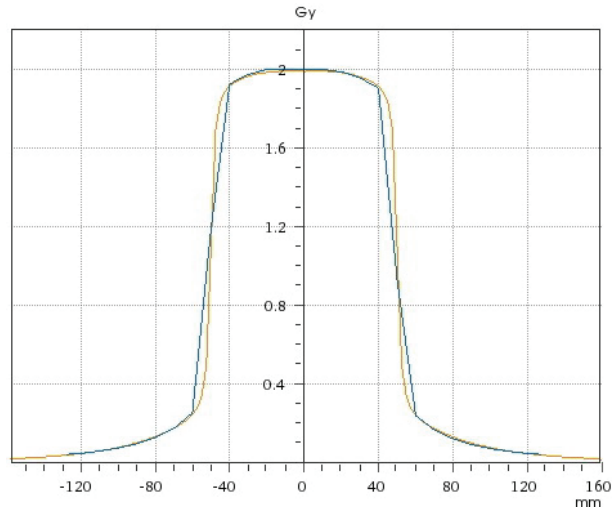


**Fig. 4** Static field 10 x 10 cm<sup>2</sup>, coronal plane, isocentric cross profile: OCTAVIUS 4D with Detector 729 (spatial resolution 10 mm, green curve) versus TPS (yellow curve). The pass rate in the complete plane was 83.3%.

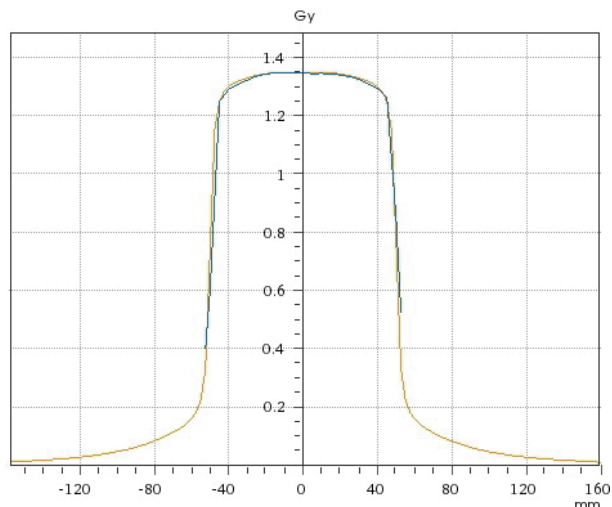


**Fig. 5** Static field, 10 x 10 cm<sup>2</sup>, coronal plane, isocentric cross profile: OCTAVIUS 4D with Detector 1000<sup>SRS</sup> (spatial resolution 2.5 mm, green curve) versus TPS (yellow curve). The pass rate in the complete plane was 100% (95.5% at 1% / 1 mm).

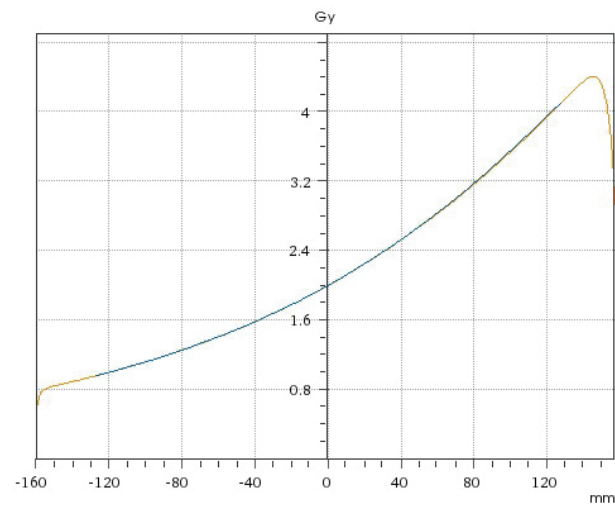


**Fig. 6** Static field, 10 x 10 cm<sup>2</sup>, transverse plane: Central axis depth dose distribution obtained by OCTAVIUS 4D with Detector 729 (green curve), compared with TPS (yellow curve). The pass rate in the complete plane was 88.3%.

#### 4.3 Comparison with a stationary detector panel and with TPS results

A more realistic test is the comparison of OCTAVIUS 4D with a system using a stationary detector panel by applying an IMRT plan or a rotational plan. For this purpose, an OCTAVIUS II system, consisting of a stationary octagonal phantom and a Detector 729, was irradiated with an IMRT Head & Neck plan consisting of 11 fields. The coronal plane defined by the detector panel was evaluated with VeriSoft. Then the same irradiation plan was applied to an OCTAVIUS 4D system, and the same coronal plane was extracted from the 3D dose grid. Fig. 7 shows the comparison of both measurements with the TPS. The OCTAVIUS II achieved a pass rate of 99.8%, while the pass rate of the OCTAVIUS 4D was 99.2%.

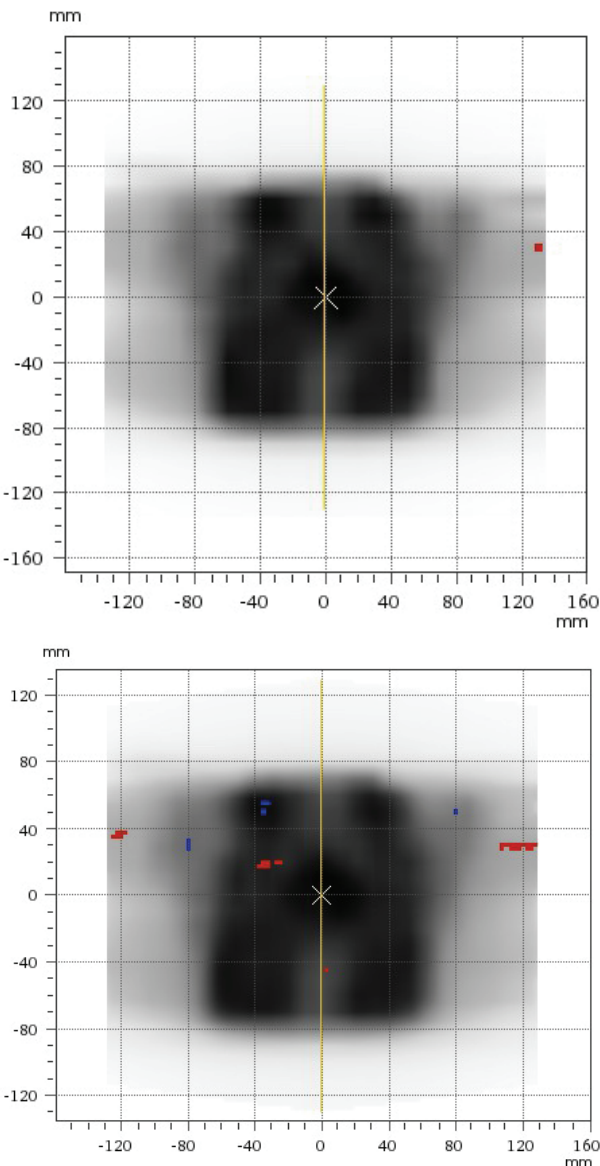


**Fig. 7** Comparison of dose values in the coronal plane obtained by a stationary OCTAVIUS II system (upper graph) and a rotational OCTAVIUS 4D system (lower graph). The irradiated plan was a Head & Neck IMRT plan with 11 fields. The pass rates were 99.8% and 99.2%, respectively.

A similar comparison between OCTAVIUS II and OCTAVIUS 4D was made by the delivery of a RapidArc lung plan with nodes. Here the pass rates were 100% for OCTAVIUS II and 99.6% for OCTAVIUS 4D.

Finally, a clinical prostate plan was measured with OCTAVIUS 4D using detector panels with different spatial resolution. Fig. 8 shows the results for the Detector 729 with 10 mm resolution and for the Detector 1000<sup>SRS</sup> with 2.5 mm resolution. At 3% / 3 mm both pass rates were 100%, therefore the criterion was changed to 2% / 2 mm. The pass rates were then 95% and 98.5%, respectively.

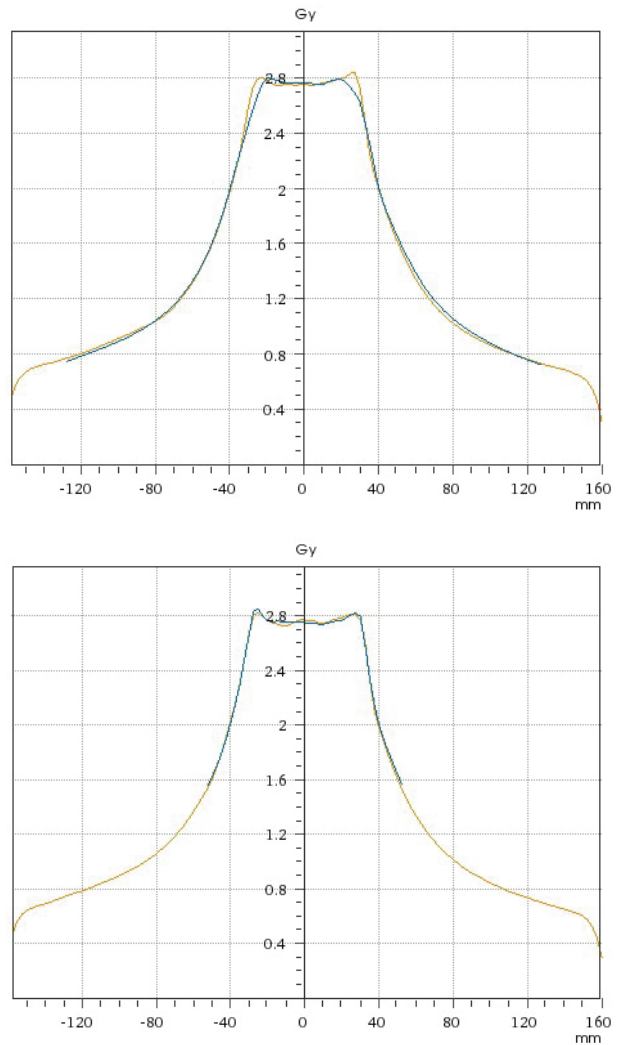


**Fig. 8** Effect of spatial resolution of the detector panel. The upper graph shows a profile in the coronal plane obtained with the Detector 729, the lower graph depicts the equivalent profile obtained with the Detector 1000<sup>SRS</sup>. Both detector panels were used with the OCTAVIUS 4D system. The corresponding TPS profiles are overlaid in yellow color. The pass rates in the complete plane for a gamma criterion of 2% / 2 mm were 95% and 98.5%, respectively.

#### 4.4 Test of DVH accuracy

The accuracy of the dose volume histograms determined by OCTAVIUS 4D has been evaluated by comparing them with DVHs exported from the treatment planning system. All measurements were made using the Detector 729. For a set

of clinical treatment plans the maximum doses were determined from the reconstructed plan and from the TPS. The differences between reconstruction and TPS were noted and their mean values calculated. The uncertainty of the maximum DVH dose measured with OCTAVIUS 4D was found to be  $\pm 2\%$  for relatively homogenous plans, and  $\pm 6\%$  for lung plans. These uncertainties are approximately twice as high as the uncertainty of the DVHs calculated by the TPS.

For a deeper insight into the accuracy of the reconstructed 3D dose grid in the patient, the commercial version of VeriSoft was modified to allow the comparison of reconstructed dose planes in the patient with those from the TPS. Fig. 9 shows the result of such a gamma analysis in a patient's plane.

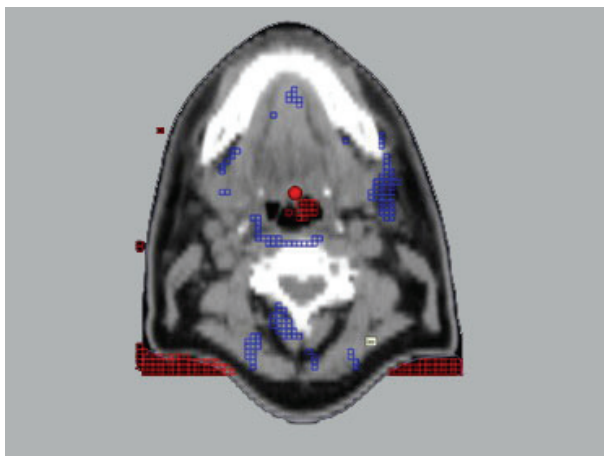


**Fig. 9** Dose plane in the patient's geometry, comparison between OCTAVIUS 4D and TPS. The red failed points at the bottom reflect the fact that the reconstruction algorithm included the air between the patient and the couch whereas the TPS did not. For this gamma analysis, the commercial version of the VeriSoft program was modified and the results compared with a Pinnacle treatment planning system. The pass rate at 2% / 2 mm was 93.3%.

In order to estimate the dose errors in the reconstructed patient, a series of gamma analyses in the complete volume was made by varying the dose criterion while keeping the distance-to-agreement criterion constant at 2 mm. From the resulting relationship between dose criterion and pass rate it could be seen that a pass rate of one standard deviation ( $k = 1$ ) corresponded to a dose error of approximately  $\pm 2\%$  for relatively homogeneous plans and  $\pm 5.5\%$  for lung plans. This is in reasonable agreement with the differences found by comparing the maximum doses as described above.

## 5 Discussion

The algorithms used by OCTAVIUS 4D are straightforward, using only the gantry-resolved measured dose matrices, the associated gantry angles, and a very limited set of additional data provided by the user upon commissioning of the system. For the dose distribution in the phantom the

additional data consist of PDDs at different field sizes and the phantom's electron density. For the dose distribution in the patient, geometric information on the patient's structures and their densities are needed in addition. No dose information from the TPS is used to establish the measured dose distributions, making the OCTAVIUS 4D system a real independent QA tool.

The biggest discrepancies between OCTAVIUS 4D and TPS data is found for cross profiles measured with the Detector 729 in static fields (Fig. 4). This is the result of the relatively coarse spatial resolution of the detector panel. The individual detectors are  $0.5 \times 0.5 \times 0.5 \text{ cm}^3$  in size and separated by 10 mm center to center. The fact that the phantom normally rotates with the beam smears out this resolution effect to a big degree, increasing the pass rate in the evaluated plane from 83.3% to 99.8%. Also, the use of a detector panel with a higher spatial resolution improves the results (Fig. 5).

The measurement of a static depth dose curve shows very good agreement with the TPS (Fig. 6). Nevertheless, the pass rate of 88.3% for the evaluated transverse plane is relatively low. This is obvious as the gamma index analysis covers not only the central axis shown in Fig. 6 but also the complete field including the penumbra regions. Again, the limited spatial resolution of the Detector 729 is responsible for this effect.

Fig. 7 compares dose distributions reconstructed by OCTAVIUS 4D and measured directly by a stationary detector panel, avoiding the need of dose reconstruction algorithms. While the stationary OCTAVIUS II system only evaluates the gamma values for each detector on the panel, the rotating OCTAVIUS 4D system calculates gamma values for all reconstructed voxels in the complete volume. The reconstruction of voxels is based on a linear interpolation between detectors which leads to small uncertainties. As a result, the pass rate of the OCTAVIUS 4D with Detector 729 is slightly lower than that of the OCTAVIUS II, especially in regions of steep dose gradients.

A comparison of OCTAVIUS 4D with head & neck plans of 50 patients has been reported in the literature [12]. The average pass rate found was  $(99.2 \pm 0.8)\%$ . These measurements included high-dose rate, flattening filter free (FFF) beams. This indicates that the OCTAVIUS 4D reconstruction algorithm works for both flattened and unflattened beams.

The data shown in Fig. 8 clearly demonstrate the fact that the pass rate for clinical treatment plans raises as the spatial resolution of the detector panel is increased.

Although the problem is much reduced by the rotation of the phantom, the spatial resolution of 10 mm for the Detector 729 and the associated linear interpolation

algorithm result in small, but detectable deficiencies in the gamma analysis. In this context, however, it is worth noting that comparable devices are having similar restrictions. The Delta-4, for instance, also uses a linear interpolation algorithm [8], and the ArcCHECK requires agreement between measurements and treatment plan within approximately 10% in order to be able to reliably correct the calculated patient dose distribution [10]. For the COMPASS system dose errors of up to 17% have been reported [9].

Finally, the treatment planning systems themselves are not free of errors. Errors in the range 1% - 3% have been reported [19], [20], [21]. In the presence of air volumes (lung) the inaccuracies of the TPS calculations can be even higher by a factor of 3 - 5 [19], [20], [21].

The uncertainty in the determination of DVHs in the patient originates from measurement inaccuracies and inaccuracies of the reconstruction algorithm used by OCTAVIUS 4D. The more homogeneous the patient structure of interest is, the better the accuracy of the reconstructed DVH. The uncertainty of the reconstructed maximum doses of the DVHs ranges from  $\pm 2\%$  for relatively homogeneous plans to  $\pm 6\%$  for lung plans. This seems to be very adequate considering the fact that no information from the TPS about the dose distribution is required by the reconstruction algorithm.

## 6 Conclusions

The OCTAVIUS 4D algorithms for the reconstruction of three-dimensional dose distributions in the phantom and in the patient have been described. The algorithms are completely independent of dose information calculated by the treatment planning system, and they need only very few basic data for the commissioning. Various validation procedures and results have been presented, proving the suitability of OCTAVIUS 4D for clinical IMRT and VMAT pre-treatment QA. Validity of the system for use with FFF beams has been reported in the literature [12]. The dose accuracy of dose volume histograms in the patient's geometry has been estimated to vary from  $\pm 2\%$  to  $\pm 6\%$  depending on the magnitude of the density variations in the patient. The accuracy of the system can be improved by the use of detector panels with higher spatial resolution such as the Detector 1000<sup>SRS</sup>.

## References

- [1] E Spezi et al., "Characterization of a 2D ion chamber array for the verification of radiotherapy treatments", *Phys. Med. Biol.* **50** (2005) 3361 - 3373
- [2] S. Cilla et al., "Portal dose measurements by a 2D array", *Physica Medica* (2007) **23**, 25 - 32
- [3] Ann Van Esch et al., "On-line quality assurance of rotational radiotherapy treatment delivery by means of a 2D ion chamber array and the Octavius phantom", *Med. Phys.* **34** (10), October 2007, 3825 - 3837
- [4] Paul A Jursinic et al., "MapCHECK used for rotational IMRT measurements: Step-and-shot, Tomotherapy, RapidArc", *Med. Phys.* **37**, (6), June 2010, 2837 - 2846
- [5] M Stasi et al., "D-IMRT verification with a 2D pixel ionization chamber: dosimetric and clinical results in head and neck cancer", *Phys. Med. Biol.* **50** (2005) 4681 - 4694
- [6] Yoichi Watanabe et al., "3D evaluation of 3DVH program using BANG3 polymer gel dosimeter", *Med. Phys.* **40** (8), August 2013, 082101-1 - 082101-11
- [7] Sotirios Stathakis et al., "Characterization of a novel 2D array dosimeter for patient-specific quality assurance with volumetric arc therapy", *Med. Phys.* **40** (7), July 2013, 071731-1 - 071731-9
- [8] R Sadagopan et al., "Characterization and clinical evaluation of a novel IMRT quality assurance system", *Journal of Applied Clinical Medical Physics*, Vol. **10**, No. 2, Spring 2009, 104 - 119
- [9] J Godart et al., "Reconstruction of high-resolution 3D dose from matrix measurements: error detection capability of the COMPASS correction kernel method", *Phys. Med. Biol.* **56** (2011), 5029 - 5043
- [10] Benjamin E. Nelms et al., "VMAT QA: Measurement-guided 4D dose reconstruction on a patient", *Med. Phys.* **39** (7), July 2012, 4228 - 4238
- [11] R Boggula et al., "Experimental verification of a commercial 3D dose verification system for intensity-modulated arc therapies", *Phys. Med. Biol.* **55** (2010), 5619
- [12] Conor K. McGarry et al., "Octavius 4D characterization for flattened and flattening filter free rotational deliveries", *Med. Phys.* **40** (9), September 2013, 091707-1 - 091707-11
- [13] PTW-Freiburg, Technical Note, "Parameter Settings in VeriSoft when relative Electron Density cannot be set in the TPS", D655.200.07
- [14] R. C. Taylor et al., "A generic off-axis correction for linac photon beam dosimetry", *Med. Phys.* **25** (5), May 1998, 662 - 667
- [15] Dietmar Georg and Gabriele Kragl, „Photon beam quality variations of a flattening filter free linear accelerator", *Med. Phys.* **37** (1), January 2010, 49 - 53
- [16] S J Thomas, "Relative electron density calibration of CT scanners for radiotherapy treatment planning", *The British Journal of Radiology*, **72** (1999), 781 - 768
- [17] "Central Axis Depth Dose Data for Use in Radiotherapy", *British Journal of Radiology*, Supplement 11, London 1972
- [18] Tom Depuydt et al., "A quantitative evaluation of IMRT dose distributions: refinement and clinical assessment of the gamma evaluation", *Radiotherapy and Oncology* **62** (2002) 309 - 319
- [19] I. Ali et al., "Quantitative assessment of the accuracy of dose calculation using pencil beam and Monte Carlo algorithms and requirements for clinical quality assurance", *Medical Dosimetry*, in press, 2013
- [20] Tao Han et al., "Dosimetric comparison of Acuros XB deterministic radiation transport method with Monte Carlo and model-based convolution methods in heterogeneous media", *Med. Phys.* **38** (5), May 2011, 2651 - 2664
- [21] M. W. K. Kan et al., "Experimental verification of the Acuros XB and AAA dose calculation adjacent to heterogeneous media for IMRT and RapidArc of nasopharyngeal carcinoma", *Med. Phys.* **40** (3), March 2013, 031714-1 - 031714-19